

The Hartman effect in graphene

Zhenhua Wu, Kai Chang, J. T. Liu, X. J. Li, and K. S. Chan

Citation: *J. Appl. Phys.* **105**, 043702 (2009); doi: 10.1063/1.3078079

View online: <http://dx.doi.org/10.1063/1.3078079>

View Table of Contents: <http://jap.aip.org/resource/1/JAPIAU/v105/i4>

Published by the [American Institute of Physics](#).

Additional information on J. Appl. Phys.

Journal Homepage: <http://jap.aip.org/>

Journal Information: http://jap.aip.org/about/about_the_journal

Top downloads: http://jap.aip.org/features/most_downloaded

Information for Authors: <http://jap.aip.org/authors>

ADVERTISEMENT

The advertisement banner for AIP Advances features a light green background with a pattern of thin, curved, wavy lines. The text "AIPAdvances" is prominently displayed in the center, with "AIP" in blue and "Advances" in green. To the right of the text is a circular seal with the text "Now Indexed in Thomson Reuters Databases". Below the main text, there is a blue horizontal bar with the text "Explore AIP's open access journal:". To the right of this bar, there is a list of three bullet points: "• Rapid publication", "• Article-level metrics", and "• Post-publication rating and commenting".

AIPAdvances

Now Indexed in Thomson Reuters Databases

Explore AIP's open access journal:

- Rapid publication
- Article-level metrics
- Post-publication rating and commenting

The Hartman effect in graphene

Zhenhua Wu,¹ Kai Chang,^{1,a)} J. T. Liu,² X. J. Li,³ and K. S. Chan^{4,b)}

¹*SKLSM, Institute of Semiconductors, Chinese Academy of Sciences, P.O. Box 912, Beijing 100083, China*

²*Department of Physics, Nanchang University, Nanchang 330031, China*

³*School of Physics and Optoelectronics Technology, Fujian Normal University, Fuzhou 350007, China*

⁴*Department of Physics and Materials Science, City University of Hong Kong, Tat Chee Avenue, Kowloon, Hong Kong, China*

(Received 9 September 2008; accepted 28 December 2008; published online 17 February 2009)

We investigate theoretically the Hartman effect in quantum tunneling through single and double barriers in a single graphene layer. The numerical results indicate that the Hartman effect in graphene depends heavily on the incident angle and the energy of the carrier in the tunneling process through single and double barriers. We find that the Hartman effect disappears for normal incidence and appears when the incident angle and energy are larger than some critical values. © 2009 American Institute of Physics. [DOI: [10.1063/1.3078079](https://doi.org/10.1063/1.3078079)]

I. INTRODUCTION

Quantum tunneling has received much attention in the past decades. A considerable number of previous studies focused on the time scale that a particle takes to tunnel through a barrier.^{1–3} The group delay time τ_g is one of the important quantities related to the dynamic aspect of the tunneling process. Hartman⁴ calculated the group delay time by analyzing wavepackets' behavior and found that the group delay time τ_g can be expressed in terms of the derivative of the phase shift with respect to energy. It is surprising to find that the group delay time τ_g for a particle tunneling through a rectangular barrier is independent of the barrier thickness provided the barrier is opaque. This phenomenon, often referred to as the Hartman effect, implies that for sufficiently large barriers the effective group velocity of the particle can become superluminal.⁵ The experimental verifications of the Hartman effect was first carried out by Enders and Nimtz⁶ in their pioneering studies. In the meantime, the superluminal group velocity has also been verified by a series of experiments measuring the delay time between the appearance of an electromagnetic pulse peak at the two sides of a barrier.^{7–10} These experiments confirm a possible explanation of the Hartman effect: the wavepacket is merely reshaped in the tunneling process. This is based on the analogy between electromagnetic tunneling of evanescent waves and quantum-mechanical tunneling because the Helmholtz equation and the Schrödinger equation in the two corresponding situations are mathematically identical.^{11–13} Recently, Winful^{14–16} also proposed another possible interpretation that the delays are not propagation delays and, therefore, the saturation of the group delay time does not imply superluminal and unlimited velocity. The delay time is associated with the momentary capture and release of a tunneling particle; thus, the origin of the Hartman effect has been traced back to the storage of particles and it can be explained on the basis of the saturation of the integrated probability density in the barrier region. Furthermore, the study of the Hartman effect is not

limited to simple structures that contain only a single rectangular barrier. The Hartman effect in structures with two or more barriers has been investigated both theoretically^{17,18} and experimentally.^{19–21} The Hartman effect in a quantum ring in the presence of an Aharonov–Bohm flux was also examined theoretically, showing that the Hartman effect exists under proper conditions.²²

Recently, graphene, which consists of carbon atoms in a two-dimensional (2D) honeycomb lattice, was fabricated utilizing micromechanical cleaving.²³ At the K (or K') point of the Brillouin zone, the electron energy spectrum exhibits a linear dispersion that can be well described by the massless Dirac equation with an effective speed of $v_F \approx 10^6$ ms⁻¹. These quasiparticles, also called massless Dirac fermions, can be viewed as electrons that lose their rest mass m_0 or as neutrinos that acquire the electron charge e .

In this paper, we study theoretically the Hartman effect in a single graphene layer, wherein the particles are described by the massless Dirac equation rather than the Schrödinger equation in conventional semiconductor structures. We find that the Hartman effect also exists in the massless Dirac fermion system. Our calculation results show that the Fermi energy and the incident angle of the particle play key roles in determining the existence of the Hartman effect in graphene.

This paper is organized as follows. In Sec. II, we present the theoretical model and the calculation method. We show and discuss the numerical results in Sec. III. Finally, we give the conclusions in Sec. IV.

II. THEORY

We consider tunneling through single and double barriers in a single layer graphene shown schematically in Fig. 1. We consider the single and double barrier structures that are rectangular in shape and infinite along the y direction. In the present study, a Dirac fermion with energy E and momentum $\hbar k$ is incident from the left side with incident angle ϕ on a potential barrier with height V_0 and thickness D . In contrast to a Schrödinger particle, a massless Dirac fermion has a linear energy dispersion $E = \hbar v_F k$ and a unique chirality.²³

^{a)}Electronic mail: kchang@red.semi.ac.cn.

^{b)}Electronic mail: apkschan@cityu.edu.hk.

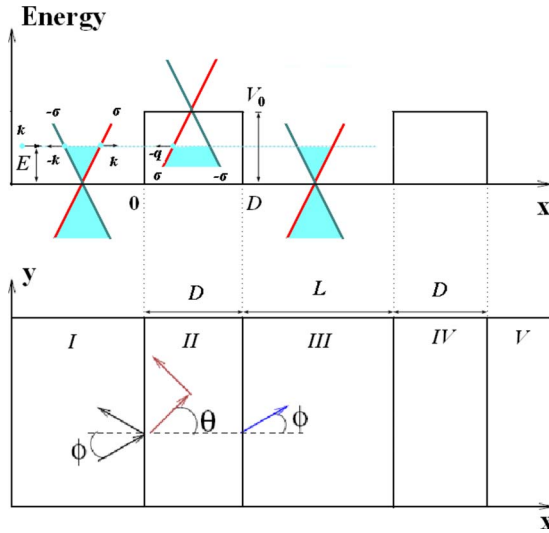


FIG. 1. (Color online) Top: Schematic showing the tunneling of an electron through a double barrier structure and the corresponding energy dispersions. The blue dotted line shows the Fermi energy level E that lies in the conduction band outside the barriers and inside the valence band in the barriers. The colors of the branches of the energy dispersion denote the pseudospin orientation, pseudospin σ being parallel (red) or antiparallel (green) to the direction of motion of electron (hole). Bottom: Definitions of the angles ϕ and θ which are the incident and refractive angles in the tunneling process.

In a single graphene layer, the carbon atoms are arranged in a hexagonal lattice. Electrons in graphene can be described by the massless Dirac equation at low energy in the two nonequivalent valleys K and K' points.²⁴ Electrons in each valley can formally be described by the massless Dirac-like Hamiltonian,^{25–27}

$$\hat{H} = \hbar v_F \begin{pmatrix} 0 & k_x - ik_y \\ k_x + ik_y & 0 \end{pmatrix} = \hbar v_F \vec{\sigma} \cdot \vec{k}, \quad (1)$$

where \vec{k} is the momentum, $\sigma_i (i=x, y)$ is the Pauli matrix, and the k -independent Fermi velocity v_F plays the role of the speed of light.

In this system, the two-component electron wave function, $\psi(\vec{r})$, is given by the 2D massless Dirac equation

$$\hat{H}\psi(\vec{r}) = \hbar v_F \vec{\sigma} \cdot \nabla \psi(\vec{r}) = E\psi(\vec{r}). \quad (2)$$

The wave function of the Dirac fermion at the K valley has the form

$$\psi(\vec{r}) = \frac{1}{\sqrt{2}} \begin{pmatrix} 1 \\ \pm e^{i\theta_k} \end{pmatrix} e^{i\vec{k} \cdot \vec{r}}. \quad (3)$$

In this paper, we focus on the situation where the energy of the incident electron E is lower than the potential barrier V_0 according to the Hartman effect.⁴ For tunneling through a single barrier, the wave functions in different regions (regions I–III shown in Fig. 1) can be written as

$$\psi_I(\vec{r}) = \frac{1}{\sqrt{2}} \begin{pmatrix} 1 \\ s e^{i\phi} \end{pmatrix} e^{i(k_x x + k_y y)} + \frac{r}{\sqrt{2}} \begin{pmatrix} 1 \\ s e^{i(\pi - \phi)} \end{pmatrix} e^{i(-k_x x + k_y y)}, \quad (4)$$

where $s = \text{sgn}(E)$, $\phi = \arctan(k_y/k_x)$, $k_x = k_F \cos \phi$, $k_y = k_F \sin \phi$, and k_F is the Fermi wave vector. In region II we have

$$\psi_{II}(\vec{r}) = \frac{a}{\sqrt{2}} \begin{pmatrix} 1 \\ s' e^{i\theta} \end{pmatrix} e^{i(q_x x + k_y y)} + \frac{b}{\sqrt{2}} \begin{pmatrix} 1 \\ s' e^{i(\pi - \theta)} \end{pmatrix} e^{i(-q_x x + k_y y)}, \quad (5)$$

here $s' = \text{sgn}(E - V_0) = -1$ (here we focus on the case that $E < V_0$), $q_x = \sqrt{(V_0 - E)^2 / v_F^2 - k_y^2}$, and $\theta = \arctan(k_y/q_x)$. In region III, we have

$$\psi_{III}(\vec{r}) = \frac{t}{\sqrt{2}} \begin{pmatrix} 1 \\ s e^{i\phi} \end{pmatrix} e^{i(k_x x + k_y y)}. \quad (6)$$

For tunneling through double barriers, we can write the comparable wave functions in different regions [see Fig. 1(b)] in a similar way. In regions I and II, $\psi_I(\vec{r})$ and $\psi_{II}(\vec{r})$ are the same as in the single barrier case. In regions III–V, we have

$$\psi_{III}(\vec{r}) = \frac{c}{\sqrt{2}} \begin{pmatrix} 1 \\ s e^{i\phi} \end{pmatrix} e^{i(k_x x + k_y y)} + \frac{d}{\sqrt{2}} \begin{pmatrix} 1 \\ s e^{i(\pi - \phi)} \end{pmatrix} e^{i(-k_x x + k_y y)}, \quad (7)$$

$$\psi_{IV}(\vec{r}) = \frac{e}{\sqrt{2}} \begin{pmatrix} 1 \\ s' e^{i\theta} \end{pmatrix} e^{i(q_x x + k_y y)} + \frac{f}{\sqrt{2}} \begin{pmatrix} 1 \\ s' e^{i(\pi - \theta)} \end{pmatrix} e^{i(-q_x x + k_y y)}, \quad (8)$$

$$\psi_V(\vec{r}) = \frac{t}{\sqrt{2}} \begin{pmatrix} 1 \\ s e^{i\phi} \end{pmatrix} e^{i(k_x x + k_y y)}. \quad (9)$$

Note that all of the above coefficients of the wave functions can be obtained from the boundary conditions.

First, we study tunneling through the single barrier and calculate two important tunneling times—the group delay time τ_g and the dwell time τ_d .²

The relationship between the group delay time and the dwell time was studied by Winful¹⁴ for a one-dimensional system. Following the same approach, we derive the group delay time τ_g and the dwell time τ_d in a 2D graphene system. The group delay time is the time delay between the appearances of the wavepacket's peak at $x=0$ and $x=D$. The group delay time τ_g is given by the energy derivative of the transmission phase shift

$$\tau_{gt} = \hbar \frac{d\phi_0}{dE}, \quad (10)$$

where $\phi_0 = \phi_t + k_x D$. The group delay time in reflection is given by

$$\tau_{gr} = \hbar \frac{d\phi_r}{dE}. \quad (11)$$

For a general asymmetric barrier, τ_{gt} and τ_{gr} differ from each other, and the group delay time τ_g is defined as

$$\tau_g = |t|^2 \tau_{gt} + |r|^2 \tau_{gr}, \quad (12)$$

while for symmetric barriers,

$$\tau_g = \tau_{gt} = \tau_{gr}. \quad (13)$$

The dwell time is the time spent by a particle in the barrier region $0 < x < D$ regardless of whether it is ultimately transmitted or reflected,

$$\tau_d = \frac{\int_0^D |\psi(x)|^2 dx}{j_{in}}, \quad (14)$$

where $\psi(x)$ is the stationary state wave function with energy E and $j_{in} = v_F \cos(\phi)$ is the flux of incident particles. The relationship between τ_g and τ_d is derived as follows. We use the probability conservation equation for a 2D Dirac system:

$$\frac{\partial \rho}{\partial t} + \nabla \cdot \vec{j} = 0, \quad (15)$$

where $\rho = \psi^\dagger(\vec{r})\psi(\vec{r})$ and $\vec{j} = v_F \psi^\dagger(\vec{r}) \vec{\sigma} \psi(\vec{r})$. Multiplying the two sides of the probability conservation equation by $i\hbar$, we get

$$\hat{H}[\psi^\dagger(\vec{r})\psi(\vec{r})] = -i\hbar v_F \nabla \cdot [\psi^\dagger(\vec{r}) \vec{\sigma} \psi(\vec{r})]. \quad (16)$$

so,

$$\psi^\dagger(\vec{r})\psi(\vec{r}) = -i\hbar v_F \nabla \cdot \left(\psi^\dagger(\vec{r}) \vec{\sigma} \frac{\partial}{\partial E} \psi(\vec{r}) \right). \quad (17)$$

Considering the translational symmetry in the y -direction, we have

$$\int_0^D |\psi|^2 dx = -i\hbar v_F \left[\left(\psi^\dagger(\vec{r}) \vec{\sigma}_x \frac{\partial}{\partial E} \psi(\vec{r}) \right)_{x=D} - \left(\psi^\dagger(\vec{r}) \vec{\sigma}_x \frac{\partial}{\partial E} \psi(\vec{r}) \right)_{x=0} \right]. \quad (18)$$

In front of the barrier, the wave function consists of an incident and a reflected component:

$$\psi_I(\vec{r}) = \frac{1}{\sqrt{2}} \begin{pmatrix} 1 \\ s e^{i\phi} \end{pmatrix} e^{i(k_x x + k_y y)} + \frac{r}{\sqrt{2}} \begin{pmatrix} 1 \\ s e^{i(\pi - \phi)} \end{pmatrix} e^{i(-k_x x + k_y y)}. \quad (19)$$

Behind the barrier, there is only a transmitted component,

$$\psi_{III}(\vec{r}) = \frac{t}{\sqrt{2}} \begin{pmatrix} 1 \\ s e^{i\phi} \end{pmatrix} e^{i(k_x x + k_y y)}. \quad (20)$$

The right-hand side of Eq. (18) becomes $\hbar v_F \cos(\phi) \times (|t|^2 d\phi_0/dE + |r|^2 d\phi_r/dE)$. From Eq. (18), we can obtain the group delay time

$$\tau_g = \frac{\int_0^D |\psi|^2 dx}{v_F \cos(\phi)} = \tau_d, \quad (21)$$

where τ_d is the dwell time defined by Eq. (14). This relationship differs from the case of Schrödinger particles where the group delay time equals the dwell time plus a self-

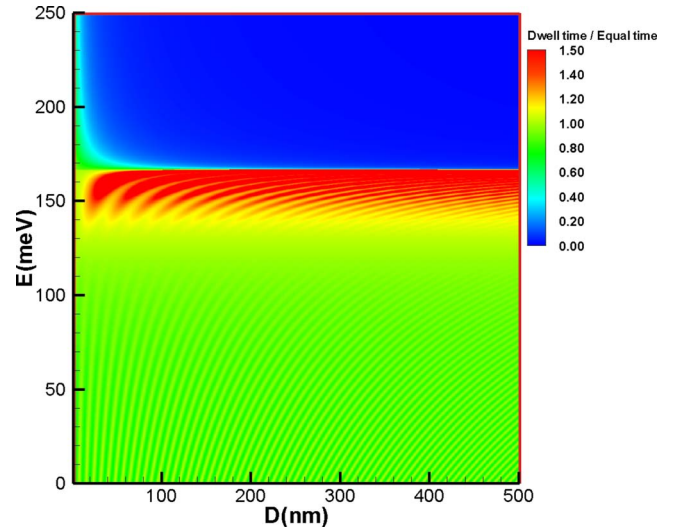


FIG. 2. (Color online) The ratio of the dwell time to the equal time as function of the barrier thickness D and the incident energy E at a certain incident angle $\phi = \pi/6$. The potential barrier height is $V_0 = 250$ meV. The critical incident energy is about $E_0 \approx 167$ meV.

interference term that comes from the overlap of the incident and reflected waves in front of the barrier (see Ref. 13). It seems that the difference stems from the different energy dispersions of the Dirac particle and Schrödinger particle.

III. NUMERICAL RESULTS AND DISCUSSIONS

To examine whether the Hartman effect exists in this system, we analyze the behavior of τ_g/τ_0 as a function of various physical parameters. τ_0 is the equal time, i.e., the time a particle would take to travel the same distance D in the absence of the barrier.

In Fig. 2, we plot τ_g/τ_0 as a function of the barrier thickness D and the energy of the incident particle E at an incident angle $\phi = \pi/6$ and a potential barrier $V_0 = 250$ meV. The figure shows that there is a critical value of E_0 . In the case that the incident energy is larger than the critical value, τ_g/τ_0 vanishes as the barrier thickness D increases. Thus, the group delay time saturates to a constant value which is independent of the barrier thickness D when the barrier thickness becomes large enough, i.e., the Hartman effect. When the incident energy is smaller than the critical value E_0 , τ_g/τ_0 oscillates with increasing barrier thickness D , which arises from the interference between the multireflections of the electron wave at different interfaces. The Hartman effect does not exist in this case since the group delay time still depends on the barrier thickness. Figure 3 plots τ_g/τ_0 as a function both of the barrier thickness D and the incident angle ϕ at an incident energy $E = 200$ meV and barrier height $V_0 = 250$ meV. Figure 3 is similar to Fig. 2, and we can also find a critical value of ϕ_0 that divides the figure into two parts. The upper part indicates that τ_g is independent of the barrier thickness, confirming the existence of the Hartman effect. In contrast, the lower part shows that τ_g oscillates and increases with the barrier thickness,; therefore the Hartman effect does not exist. In Fig. 4, we plot the phase diagram that shows clearly where the Hartman effect exists.

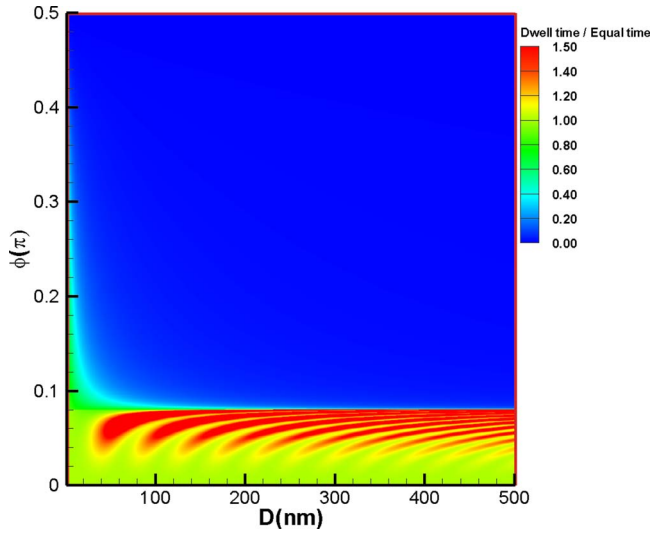


FIG. 3. (Color online) The same as Fig. 2, but now as function of the barrier thickness D and the incident angle ϕ when the incident energy $E = 200$ meV and the barrier height $V_0 = 250$ meV. The critical incident angle is $\phi_0 \approx 0.08\pi$.

Why do the incident energy E and incident angle ϕ play such important roles for the existence of the Hartman effect? This is related to the component of the wave vector q_x along the x -direction in the barrier region, which is noted in Eq. (5). E and ϕ determine whether q_x is real or imaginary. An imaginary q_x corresponds to an evanescent mode, which decays exponentially with distance across the barrier region. Consequently, the integrated probability density of the particles in the large thickness limit becomes insensitive to the barrier thickness D , i.e., the Hartman effect.

Next we turn to consider the tunneling process through the double barrier structures. Our calculation shows that the group delay time τ_g exhibits similar behavior to that for the single barrier case. The oscillation of the group delay time τ_g becomes significant since there are more interfaces in the double barrier structure, which lead to strong interference (see Figs. 5 and 6). We also plot the group delay time τ_g as a function of the distance L between the barriers for different energies and incident angles (see Fig. 7). Figure 7 indicates

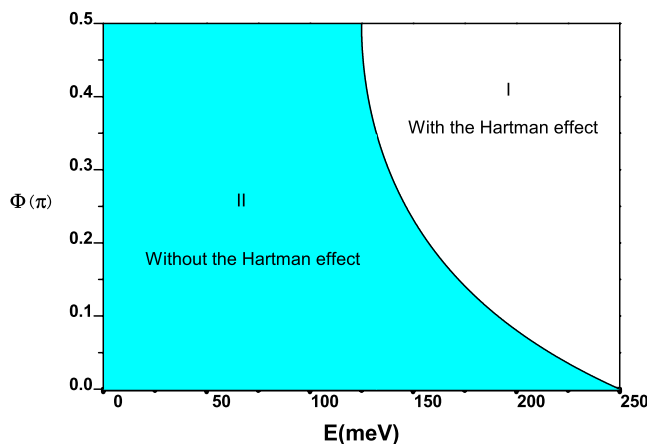


FIG. 4. (Color online) The phase diagram as a function of the incident energy E and incident angle ϕ of the particle, indicating the existence of the Hartman effect.

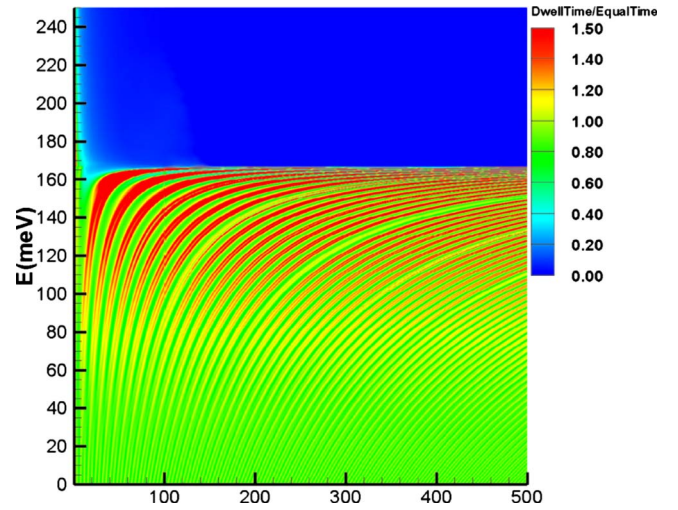


FIG. 5. (Color online) The same as Fig. 2, but now for tunneling through the double barrier structure. The distance between the two barriers is fixed at 10 nm. The critical incident energy is $E_0 \approx 167$ meV.

that the Hartman effect does not exist for normal incidence and appears (disappears) when the energy is larger (smaller) than the critical value. Note that the group delay time saturates as the distance L increases when the energy is higher than the critical value. This is because the group delay time is dominantly determined by the time spent in the area between the two barriers when the distance becomes large. The phase diagram describing the existence of the Hartman effect for the double barrier structures is the same as that for the single barrier case because the boundary in the phase diagram is determined by the wave vector of the electron in the barrier regions, i.e., the imaginary wave vector q_x .

Finally, we estimate the tunneling time for the Schrödinger and Dirac fermions in conventional semiconductors and graphene. For example, we consider the tunneling process through a single barrier GaAs/AlGaAs/GaAs structure, $m^* = 0.07m_0$, where m_0 is the bare mass of the electron, the barrier height is $V_0 = 250$ meV, the barrier thickness

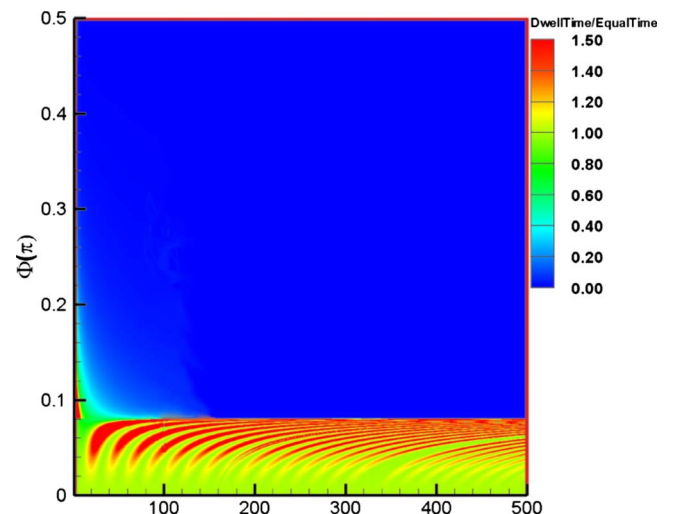


FIG. 6. (Color online) The same as Fig. 3, but now for tunneling through the double barrier structure. The distance between the two barriers is fixed at 10 nm. The critical incident angle is $\phi_0 \approx 0.08\pi$.

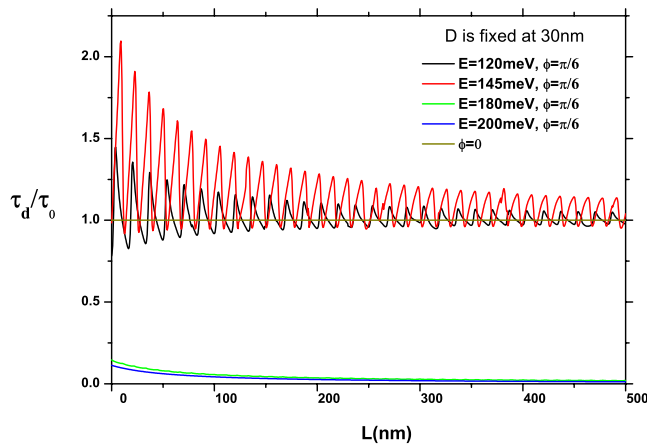


FIG. 7. (Color online) The ratio of the dwell time to the equal time as a function of the distance L between the barriers at a certain incident angle $\phi = \pi/6$. The potential barrier height is $V_0 = 250$ meV, and its thickness D is fixed at 30 nm.

is $D = 6$ nm, and the incident energy is $E = 100$ or 50 meV, respectively. The typical equal time is approximately 2.7×10^{-15} or 4.1×10^{-15} s, respectively. The velocity of an electron in a single graphene layer is independent of the in-plane momentum and/or Fermi energy ($v_F = 10^6$ m/s) and the typical equal time τ_0 is 6×10^{-15} s. The above figures demonstrate that the group delay time of the tunneling process in graphene is also approximately in the same timescale as that in conventional semiconductor tunneling devices.

IV. CONCLUSION

We investigate theoretically the Hartman effect in the tunneling processes of the massless Dirac fermion in graphene. Unlike the situation of a Schrödinger fermion, our theoretical results show that the Hartman effect exists in graphene for a specific range of incident angles ϕ and energy E of the Dirac fermion and disappears in the normal incidence case. Similar behavior of the group delay time is obtained for tunneling through the double barrier structures. Note that the group delay time is almost independent of the distance between the two successive barriers and exhibits the same phase diagram as that for the single barrier case. Our theoretical investigation on the tunneling time could be interesting for both the basic physics and the potential application of graphene based electronic devices.

ACKNOWLEDGMENTS

This work is partly supported by NSFC Grant No. 60525405 and a grant from the Research Grants Council of the Hong Kong Special Administrative Region, China Project No. CityU 100305.

- ¹Th. Martin and R. Landauer, *Phys. Rev. A* **45**, 2611 (1992).
- ²E. H. Hauge and J. A. Støvneng, *Rev. Mod. Phys.* **61**, 917 (1989).
- ³M. Büttiker, *Phys. Rev. B* **27**, 6178 (1983).
- ⁴T. E. Hartman, *J. Appl. Phys.* **33**, 3427 (1962); see also J. R. Fletcher, *J. Phys. C* **18**, L55 (1985).
- ⁵V. S. Olkhovsky and E. Recami, *Phys. Rep.* **214**, 339 (1992); V. S. Olkhovsky, E. Recami, F. Raciti, and A. K. Zaichenko, *J. Phys. I* **5**, 1351 (1995). So far, besides the pioneering work mentioned in Ref. 4 based on the stationary-phase method, many researches that analyze the tunneling times in modern forms have been done. For more details, see the review article, V. S. Olkhovsky, E. Recami, and J. Jakiel, *Phys. Rep.* **398**, 133 (2004).
- ⁶A. Enders and G. Nimtz, *J. Phys. I* **2**, 1693 (1992); **3**, 1089 (1993).
- ⁷A. M. Steinberg, P. G. Kwiat, and R. Y. Chiao, *Phys. Rev. Lett.* **71**, 708 (1993).
- ⁸Ch. Spielmann, R. Szipocs, A. Stingl, and F. Krausz, *Phys. Rev. Lett.* **73**, 2308 (1994).
- ⁹Ph. Balcou and L. Dutriaux, *Phys. Rev. Lett.* **78**, 851 (1997).
- ¹⁰V. Laude and P. Tourniois, *J. Opt. Soc. Am. B* **16**, 194 (1999).
- ¹¹A. P. L. Barbero, H. E. Hernandez-Figueroa, and E. Recami, *Phys. Rev. E* **62**, 8628 (2000).
- ¹²E. Recami, *Found. Phys.* **31**, 1119 (2001).
- ¹³E. Recami, M. Zamboni-Rached, K. Z. Nobrega, C. A. Dartora, and H. E. Hernandez, *IEEE J. Sel. Top. Quantum Electron.* **9**, 59 (2003).
- ¹⁴H. G. Winful, *Phys. Rev. Lett.* **91**, 260401 (2003).
- ¹⁵H. G. Winful, *Opt. Express* **10**, 1491 (2002).
- ¹⁶H. G. Winful, *Phys. Rev. Lett.* **90**, 023901 (2003).
- ¹⁷Y. Aharonov, N. Erez, and B. Reznik, *Phys. Rev. A* **65**, 052124 (2002).
- ¹⁸V. S. Olkhovsky, E. Recami, and G. Salesi, *Europhys. Lett.* **57**, 879 (2002); E. Recami, *J. Mod. Opt.* **51**, 913 (2004); V. S. Olkhovsky, E. Recami, and A. K. Zaichenko, *Europhys. Lett.* **70**, 712 (2005).
- ¹⁹G. Nimtz, A. Enders, and H. Spieker, *J. Phys. I* **4**, 565 (1994).
- ²⁰H. M. Brodowsky, W. Heitmann, and G. Nimtz, *Phys. Lett. A* **222**, 125 (1996).
- ²¹S. Longhi, P. Laporta, M. Belmonte, and E. Recami, *Phys. Rev. E* **65**, 046610 (2002).
- ²²S. Bandopadhyay, R. Krishnan, and A. M. Jayannavar, *Solid State Commun.* **131**, 447 (2004).
- ²³A. H. Castro Neto, F. Guinea, N. M. R. Peres, K. S. Novoselov, and A. K. Geim, *Rev. Mod. Phys.* **81**, 109 (2009); arXiv:cond-mat/0709.1163, and references therein.
- ²⁴A. K. Geim and K. S. Novoselov, *Nature Mater.* **6**, 183 (2007).
- ²⁵J. C. Slonczewski and P. R. Weiss, *Phys. Rev.* **109**, 272 (1958).
- ²⁶G. W. Semenoff, *Phys. Rev. Lett.* **53**, 2449 (1984).
- ²⁷F. D. M. Haldane, *Phys. Rev. Lett.* **61**, 2015 (1988).